Geophysical Prospecting, 2009, **57**, 543–557 doi: 10.1111/j.1365-2478.2009.00808.x

Toward a full multiscale approach to interpret potential fields

Federico Cella[1*], Maurizio Fedi[2] and Giovanni Florio[2]

[1] *Università degli Studi della Calabria, Dipartimento di Scienze della Terra, Corso Bucci, 87036 Rende (CS), Italy, and* [2] *Università di Napoli Federico II, Dipartimento di Scienze della Terra, Largo san Marcellino 10, 80138 Napoli, Italy*

Received May 2008, revision accepted March 2009

ABSTRACT

The way potential fields convey source information depends on the scale at which the field is analysed. In this sense a multiscale analysis is a useful method to study potential fields particularly when the main field contributions are caused by sources with different depths and extents. Our multiscale approach is built with a stable transformation, such as depth from extreme points. Its stability results from mixing, in a single operator, the wavenumber low-pass behaviour of the upward continuation transformation of the field with the enhancement high-pass properties of *n*-order derivative transformations. So, the complex reciprocal interference of several field components may be efficiently faced at several scales of the analysis and the depth to the sources may be estimated together with the homogeneity degrees of the field. In order to estimate the source boundaries we use another multiscale method, the multiscale derivative analysis, which utilizes a generalized concept of horizontal derivative and produces a set of boundary maps at different scales. We show through synthetic examples and application to the gravity field of Southern Italy that this multiscale behaviour makes this technique quite different from other source boundary estimators.

The main result obtained by integrating multiscale derivative analysis with depth from extreme points is the retrieval of rather effective information of the field sources (horizontal boundaries, depth, structural index). This interpretative approach has been used along a specific transect for the analysis of the Bouguer anomaly field of Southern Apennines. It was set at such scales, so to emphasize either regional or local features along the transect. Two different classes of sources were individuated. The first one includes a broad, deep source with lateral size of 45∼50 km, at a depth of 13 km and having a 0.5 structural index. The second class includes several narrower sources located at shallowest depths, ranging from 3–6 km, with lateral size not larger than 5 km and structural indexes ranging from 1–1.5. Within a large-scale geological framework, these results could help to outline the mean structural features at crustal depths.

INTRODUCTION

Potential fields are due to complex distributions of sources related to susceptibility and mass density variations for magnetic and gravity fields respectively. The estimation of the most representative features (depth, size, shape, etc.) of a buried source of potential fields is often prevented from the difficulty of isolating its own effect by the interfering effects of the nearby sources.

Attempts to remove these interfering effects may be based on information inferred from geology or geophysics. When such information lacks, mathematical methods may be used treating the measured field as a superposition of effects,

* E-mail: f.cella@unical.it

depending on sources having different spatial extents and depths. These effects are commonly separated by: a) expanding the field in some series of predetermined mathematical functions, such as trigonometric, wavelets or others, b) muting the coefficients of the unwanted effects and c) finally reconstructing the residual field from the modified set of coefficients. The main drawback of this approach arises from the difficulty to carefully evaluate the physical consistency of the single terms of the series used at step a).

This means that filtering techniques based on a pure mathematical basis can only approximately adapt to the real physical world. Distortions may occur, as when anomalies are erroneously split in two or more separated components. Such splitting may also distort the nearby or concurrent anomalies in an unpredictable way.

A completely different way to put in evidence the effects related to different scales is based on using methods based on the use of spatial field derivatives. They provide in fact a scale and depth control, through their inherent ability to filter out deep source or large-scale effects. Note that in this context the reduction of the large-scale effects is not obtained by muting but simply by powering the local effects with respect to the large-scale ones. On the other hand, some instability may occur for high-order derivatives, since any kind of noise or non-harmonic signal will be correspondingly enhanced. Stabilized derivatives such as integrated second vertical derivative (Fedi and Florio 2001) may help to reduce the enhancement of noise (Fedi and Florio 2002). Integrated second vertical derivative combines the use of a smoothing filter (the vertical integration filter) and the finite-differences method, which is much more stable than using Fourier horizontal derivatives operators. This allows a lower degrading of the signal-to-noise ratio than the standard Fourier method, especially when the order of computed derivatives increases. In any case, the best results are obtained using mixed upward continuation-derivative transformations, which may be designed to maintain physically reliable enhancements of the measured field at a reasonable signal-to-noise ratio. In fact these filters have in general a band-pass filter response. As an example, Fig. 1 shows the filter shape for two different continuation altitudes (6 and 12 sampling step) and for a differentiation order of 5. It is shown that, at higher altitudes, the smoothing effect of the continuation assimilates the filter shape to that of a band-pass filter. Thus, since varying the altitude means changing the scale at which the potential field is analysed, a suitable definition of this frequency response may consistently allow a high-resolution multiscale analysis of potential fields.

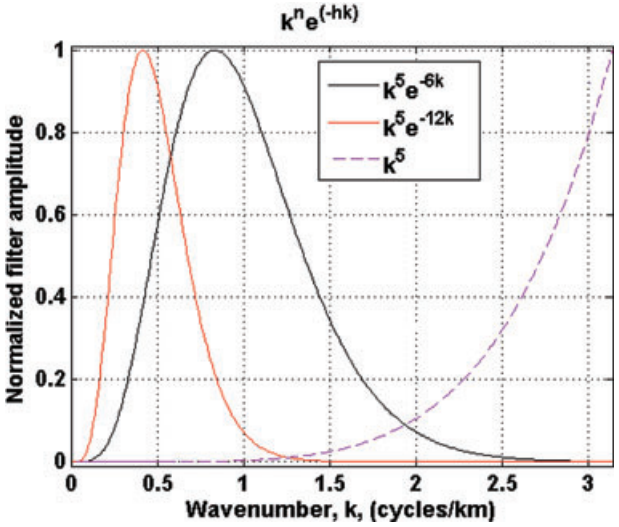

Figure 1 The composite upward continuation-vertical derivative operator. The frequency response of such composite filter for continuation altitudes $h = 6$ and 12 step units and for derivation orders $n = 5$ is shown. Such a composite filter has the shape of a band-pass filter with a central frequency higher as the derivation order increases. For reference, the frequency response of the simple fifth-order differentiation is also shown (dashed line).

The multiscale methods, which we will utilize throughout this paper, are heavily founded on the use of various-order derivatives, either vertical or horizontal. Our goal is to obtain independent information about the sources, which can be useful as itself or as the first step of interpretation. To do this, we need simple assumptions about the sources: they are considered steep enough at their boundaries to allow the field horizontal derivatives to be informative of the source horizontal extent and roughly similar to one of a large set of simple, idealized sources including spheres, cylinders, dykes, contacts or sills to satisfy the simplified theory of homogeneous fields. Whether real sources meet better the first or second type of assumption is not a simple matter but we will show that the integration of methods based on the above very simple assumptions can provide independent and valuable information about the unknown source distribution.

FIRST STEP: MULTISCALE DERIVATIVE ANALYSIS

The horizontal derivative of potential fields has long been used to image the boundaries of potential field sources (Blakely and Simpson 1986). It is based on the consideration that most

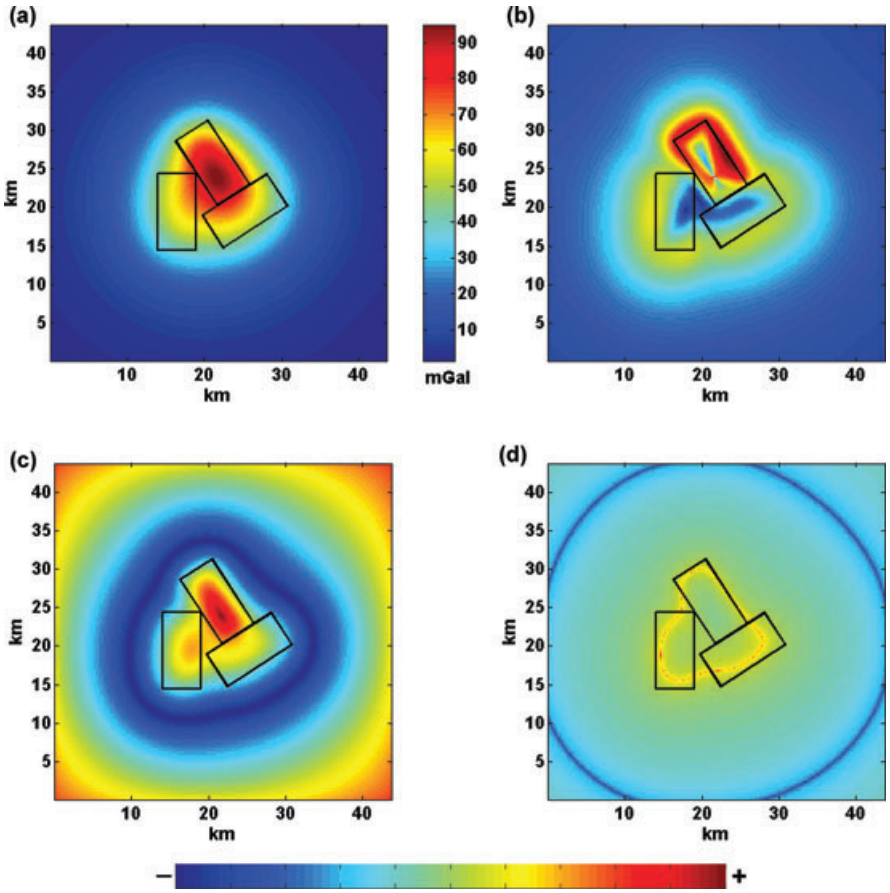

Figure 2 a) Gravity field generated by three close prismatic sources with different depths and magnetization directions. The northernmost have the top at a 2 km depth; the others are at a 4 km depth. Normalized derivatives of the reduced to the pole magnetic field, b) total horizontal derivative of the tilt angle map, c) Theta map, d) hyperbolic tiltangle map.

sources of potential fields may be modelled as a steep source, so generating strong values for the horizontal derivatives at the source boundaries.

A number of newer techniques based on the same hypothesis were recently defined, following the concept of normalized derivatives, e.g., total horizontal derivative of the tilt angle (Verduzco *et al.* 2004), hyperbolic tilt angle (Cooper and Cowan 2006), Theta map (Wijns, Perez and Kowalczyk 2005). One of the main properties shared by these functions is that they behave like an automatic gain control filter because they tend to equalize the amplitude of transformed total field magnetic anomalies. All of these functions should be applied to the total field reduced to the pole. The efficiency of these techniques is described in Fig. 2 where the test field is the gravity anomaly due to three prisms being very close to each other, having the same thickness but with different depths to the top and directions of magnetization (Fig. 2a).

The total horizontal derivative of the tilt angle (TDR_THDR) of the total field f is defined as follows:

$$TDR\_THDR = \sqrt{\left(\frac{\partial TDR}{\partial x}\right)^2 + \left(\frac{\partial TDR}{\partial y}\right)^2}, \quad (1)$$

where:

$$TDR = \arctan\left[\frac{\frac{\partial f}{\partial z}}{\sqrt{\left(\frac{\partial f}{\partial x}\right)^2 + \left(\frac{\partial f}{\partial y}\right)^2}}\right]. \quad (2)$$

The maximum values of the total horizontal derivative of the tilt angle give the estimate of the location of the source body edges (Fig. 2b).

The hyperbolic tilt angle (HTA) function is defined as:

$$HTA = \Re\left(\operatorname{arctanh}\left(\frac{\partial f/\partial z}{\sqrt{\left((\partial f/\partial x)^2 + (\partial f/\partial y)^2\right)}}\right)\right). \quad (3)$$

The maximum values of hyperbolic tilt angle give the location of the body edges. However, the existence of a negative contour on the outside of the edges of the causative bodies (Fig. 2d) represents an unwanted feature that could complicate the interpretation.

The Theta function is expressed as the horizontal derivative-to-analytic signal amplitude ratio:

$$Theta = \arccos\left(\frac{\sqrt{\left((\partial f/\partial x)^2 + (\partial f/\partial y)^2\right)}}{\left((\partial f/\partial x)^2 + (\partial f/\partial y)^2 + (\partial f/\partial z)^2\right)}\right). \tag{4}$$

The maxima of the Theta map mark the central part of the causative structures whereas the lateral boundaries are outlined by minima (Fig. 2c).

It is interesting to note that all these methods tend to convey in the same map the boundary information from structures at all scales and depths and with the same relative importance. Hence, they give the best performance when a single scale is dominant, such as in archaeological surveys for instance.

A quite different approach is based on a generalized concept of horizontal derivative, named enhanced horizontal derivative (Fedi and Florio 2001). Enhanced horizontal derivative (EHD) is a high resolution boundary estimator based on the horizontal derivative of a weighted sum of total field vertical derivatives:

$$EHD(x, y) = \sqrt{\left[\left(\frac{\partial \phi(x, y)}{\partial x}\right)^2 + \left(\frac{\partial \phi(x, y)}{\partial y}\right)^2\right]}, \tag{5}$$

where:

$$\phi(x, y) = w_0 f(x, y) + w_1 f^{(1)}(x, y) + w_2 f^{(2)}(x, y) + \ldots + w_m f^{(m)}(x, y), \tag{6}$$

and $f^{(1)}, \ldots, f^{(m)}$ are the m-order horizontal derivatives of the field f; $w_0 \ldots \ldots w_m$ is a set of weights that controls in equation (6) the relative influence of the single terms in the summation. Their careful choice allows enhancement of the lineaments related to the single involved scales. A suitable rule was suggested to this task by Fedi (2002):

$$w_i = c^i, \qquad i = 0, \ldots, m, \tag{7}$$

where m is the derivative order and c is a suitable constant.

By adding higher-order vertical derivative terms a better detail of the shallower sources is obtained, while the set of weights controls the relative importance of the terms of the summation. Of course, the use of the highest order vertical derivatives is in practice limited by the data sampling step. In general, when the derivation order gets too high for a specific data set, a further derivation does not improve anymore the spatial resolution. See Fedi and Florio (2001) for further details. Obviously, just like any other edge detector, enhanced horizontal derivative cannot be applied to some classes of sources (those approximated by spheres or infinitely long cylinders), whose boundary positions are not recoverable.

Enhanced horizontal derivative can be defined with a great flexibility as a function of the noise characteristics of the field to be analysed and, more interestingly, as a function of the wanted detail. For example, the low-order terms may also include the first vertical integral of the field and the relative enhanced horizontal derivative will allow regional-scale structures to be imaged. Due to this feature, enhanced horizontal derivative was used by Fedi (2002) to design a specific tool (multiscale derivative analysis) yielding meaningful maps of structural lineaments relative to different scales, from the regional to the local one, without performing any subjective separation of the potential fields. In the magnetic case, multiscale derivative analysis performs better for reduced to the pole magnetic anomalies.

As an example, Fig. 3 shows the multiscale derivative analysis results arising for the same gravity field of Fig. 2(a). They are compared to those of Figs 2(b), 2(c) and 2(d) deriving from normalized derivatives that, as already said, convey into a single source-boundary map the information from effects at different scales. Multiscale derivative analysis is instead a multiscale method, so allowing estimates of the source boundaries to be obtained at different scales.

As shown in Fig. 3(a), the low resolution multiscale derivative analysis map (corresponding to equations (5) and (6) starting from the potential up to the first vertical derivative) provides results similar to the Theta map (Fig. 2c). The intermediate resolution multiscale derivative analysis (Fig. 3b), corresponding to equations (5) and (6) starting from the potential up to the second vertical derivative, allows instead a description of each one source boundary more precisely than total horizontal derivative of the tilt angle map (Fig. 2b) and hyperbolic tilt angle map (Fig. 2d). Finally, the high-resolution multiscale derivative analysis map (obtained by computing enhanced horizontal derivative starting from the magnetic field up to the fourth vertical derivative in equations (5) and (6)) significantly enhances only the shallowest features of the sources (Fig. 3c), i.e., in our case those related to the northernmost source.

We can conclude that the best quality of multiscale derivative analysis is that it can provide a separated description of the source boundaries at different scales.

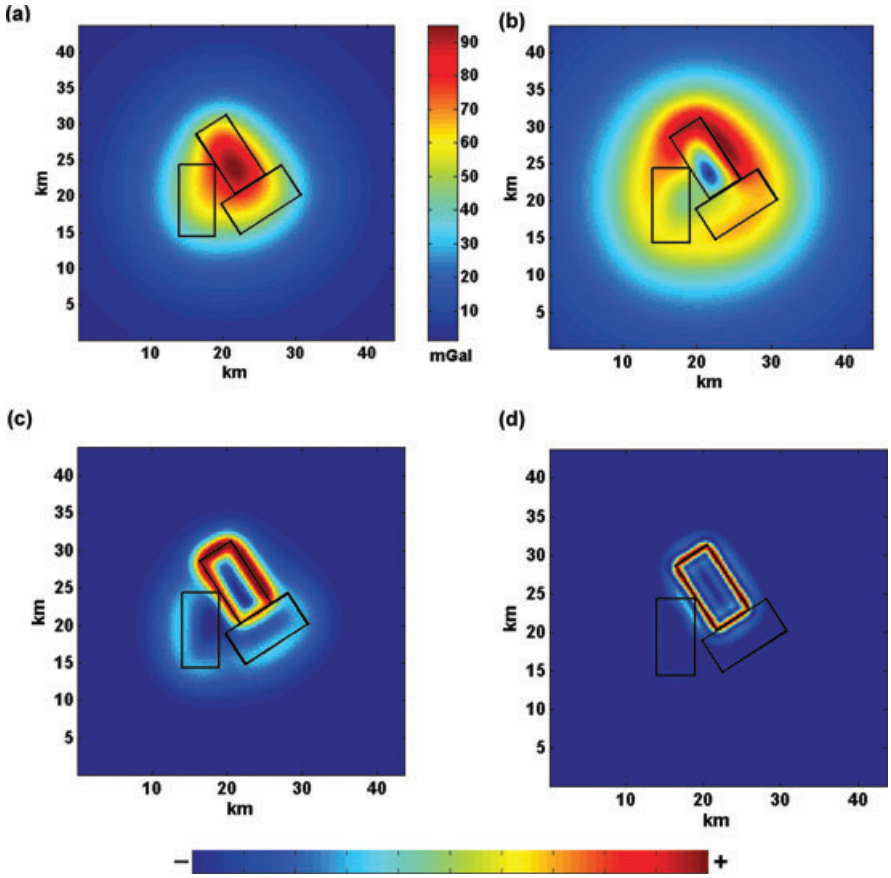

Figure 3 a) Gravity field generated by three close prismatic sources as in Fig. 2. Multiscale derivative analysis; b) enhanced horizontal derivative computed with derivatives up to the second-order (large-scale); c) enhanced horizontal derivative computed with derivatives up to the third-order (intermediate scale); d) enhanced horizontal derivative computed with derivatives up to the fourth-order derivative (short scale). Lineaments are defined by trends of local maxima that are graphically determined by the colour bar shown.

SECOND STEP: MULTILEVEL METHODS FOR SOURCE CHARACTERIZATION: THE SCALE FUNCTION AND THE DEPTH FROM EXTREME POINTS TRANSFORMATION

Our integrated approach is based, as its second step, on the use of multiscale method allowing estimates of source parameters, such as depth from extreme points (Fedi 2007), Eulz (Euler deconvolution along vertical derivatives; Florio and Fedi 2006) and scale function method (Fedi and Florio 2006). They provide estimates of source depth, density contrast and structural index in either an independent or simultaneous way. The main property of these methods is their great stability, because they take advantage of the regular behaviour of potential field data versus the altitude z. They can be applied to anomalies with rather low signal-to-noise ratios and to n-order vertical and horizontal derivatives of the analysed field. This is useful:

a) to reduce mutual interference effects and to obtain meaningful representations of the distribution of sources versus depth, with no pre-filtering;

b) to allow interpretation of the field at different scales, thanks to the different detail and inherent separation effect owning to different order derivatives.

Let us define f_1 as the Newtonian potential and any of its directional derivative $f_n (n>1)$ as:

$$f_n = \frac{\partial^{n-1} f_1}{\partial t^{n-1}}, \tag{8}$$

where t is the unit-vector along any direction in the 3D space.

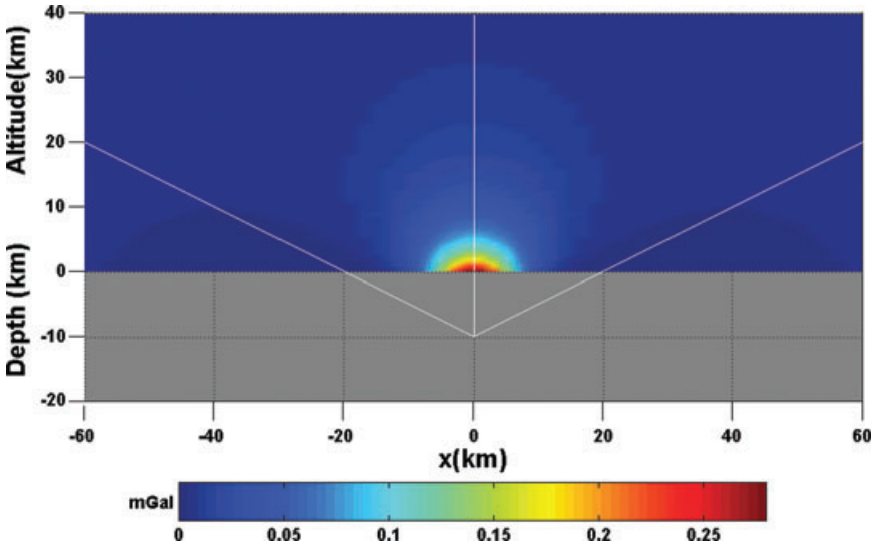

Figure 4 Vertical section of the magnetic field from upward continuation of the gravity field due to a sphere having the following features: radius = 1 km; depth 10 km; density contrast = 1/g·cm^3. Also shown, the straight lines defined by the field maxima, called 'ridges' (white solid lines). As a consequence of the dilation of potential fields versus the altitude, the ridges converge towards the singular point position (source) so forming cone-like structures.

Following Fedi (2007), consider now any n-order vertical derivative of the Newtonian potential of a pole source at $Q(x_0, y_0, z_0<0)$ at points $x = x_0$, $y = y_0$, $z>0$:

$$f_n(z) = \frac{1}{(z - z_0)^{n+1}}. \tag{9}$$

As a consequence of the dilation of potential fields versus the altitude, the field absolute values develop their maxima as straight lines (ridges) (Fig. 4) converging towards the singular pole position (source) and so forming cone-like structures. Fedi (2007) proposed to analyse potential fields at several scales with the scale function τ_n, which is defined as:

$$\tau_n = \frac{\partial \log f_n}{\partial \log z} = -\frac{S_n z}{z - z_0}, \tag{10}$$

where S_n is the structural index or the opposite of the homogeneity degree $n+1$. Throughout this paper S_1 will indicate the structural index for the gravity case, S_2 for the magnetic case, S_3 for the first-order derivatives of the magnetic field or the second-order derivatives of the gravity field and so on for higher values of n. The scale function is therefore a function of the depth to source z_0, of S_n and of the altitude z.

The depth from extreme points transformation of order n of the potential field (Fedi 2007) is defined as:

$$W_n(z) = z^{\alpha_n} f_n(z), \tag{11}$$

where z is the altitude, f_n is a potential field of order n and $\alpha_n = S_n/2$ is the scale exponent. The important property of depth from extreme points is that for any given depth source z_0, W_n has meaningful extreme points at $z = -z_0$. The depth from extreme points theory applies not only to pole (or dipole) sources but, as well as Euler deconvolution, assumes that the real sources are approximated by semi-infinite solids or volume-less figures. Each causative body is assigned to a class of simple sources with pre-fixed form, depending on its shape. As an example, concentric spheres of equal mass are all equivalent to a point-mass at their centre. Vertical/horizontal cylindrical structures (describing pipes, ridges, valleys, tunnels, volcanic necks) are close to line-models. Vertical/horizontal planar structures (describing sills, dikes, steps) are equivalent to plane-models. They may be defined as one-point sources (Stavrev 1997) because they are defined by the coordinates of just one singular point (centre, edge, vertex point) of the real figure. Previous papers (Fedi and Florio 2006; Fedi 2007) showed that depth from extreme points and scale function methods are suitable to interpret the homogeneous fields produced by such simple, one point, sources. Thus, just as Euler deconvolution, these methods are expected to give approximated yet meaningful results when applied to real cases, where the occurrence of non homogeneous fields produced by complex sources is not the exception. Because of its stability, the depth from extreme points transformation can be applied to rather high-order derivatives of potential fields, thus improving resolution of the estimates of source parameters for the multisource case.

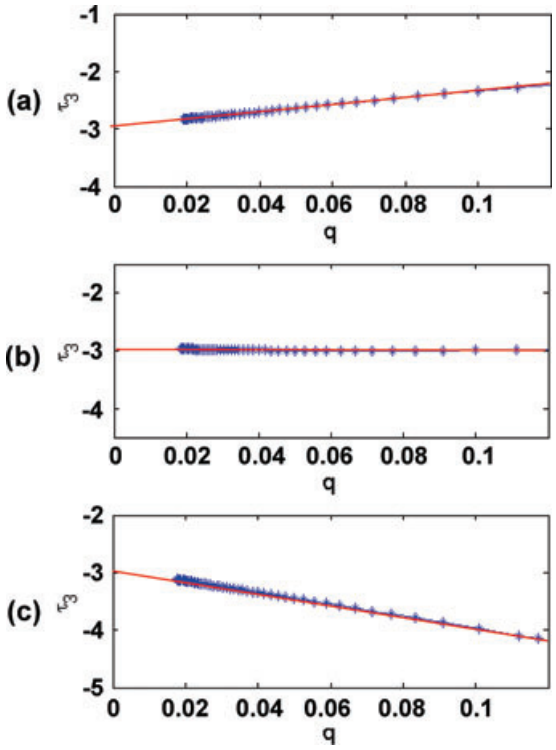

Figure 5 The scale function as a tool to determine the structural index. The rescaled scale function S_3 of a point source is a decreasing, increasing or constant function of q, respectively for $\hat{z}_0$ greater than (a), lower or equal to the true depth $z_0 = -5$ km (equation (11). A right estimate $S_3 = 4$ is given by the intercept of S_3(a, b, c).

We may rewrite equation (10) by putting $z = 1/q$, so that τ_n becomes a function of q:

$$\tau_n(q) = -\frac{S_n}{1 - z_0 q}. \tag{12}$$

$\tau_n(q)$ enjoys the useful property (Fedi 2007):

$$T_n(q \to 0) = -S_n. \tag{13}$$

Therefore, the intercept of τ_n versus q will give an estimate of the structural index S_n. Note that this estimate does not depend on z_0. Since the altimetry zero-level is arbitrary, the altitudes may be rescaled as z–$\hat{z}_0$, so that, for any given guess $\hat{z}_0$, the corresponding rescaled scale function:

$$\tau_n(q, \hat{z}_0) = -\frac{S_n(1 - \hat{z}_0 q)}{1 - z_0 q} \tag{14}$$

is an increasing, decreasing or constant function of q, respectively for $\hat{z}_0$ greater, lower or equal to the true z_0 (Fig. 5). Hence the depth to the source may also be estimated by looking at the value of $\hat{z}_0$ producing a zero-slope for τ_n.

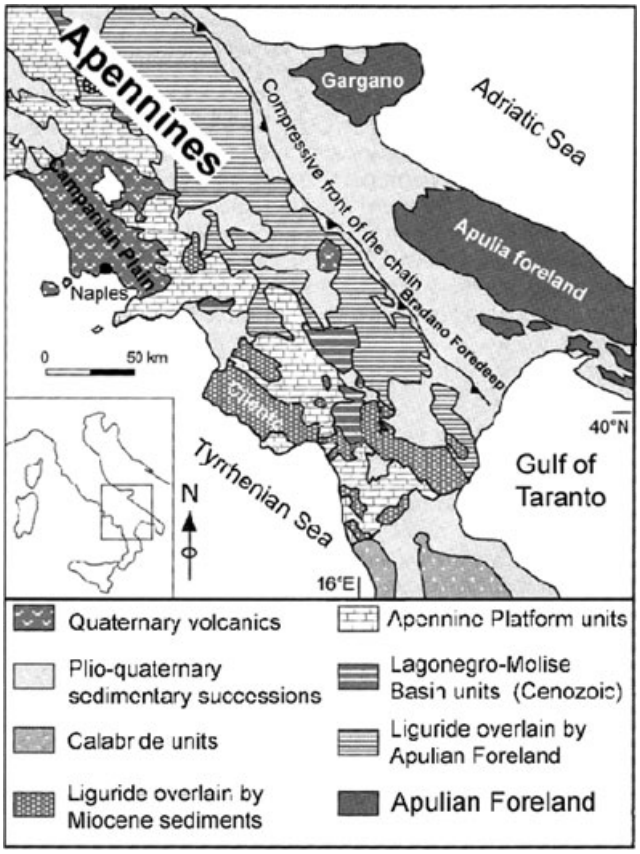

Figure 6 Sketch of the simplified geological map of the southern Apennines (modified from Parotto and Praturlon 2004).

FULL MULTISCALE INVESTIGATION OF THE SOUTHERN ITALY GRAVITY FIELD

The above properties of the scale function integrate well with multiscale derivative analysis in yielding, at different scales, a comprehensive interpretation of the field sources in terms of boundaries, depth to source, structural index. We here use such a multiscale full approach (integrated use of multiscale derivative analysis and depth from extreme points techniques), to interpret the Bouguer anomaly map of the Southern Italian region.

Geological setting

The Central-Southern sector of the Apennine chain is a complex thrust and fold belt system, built from Lower Cretaceous to Quaternary, as consequence of the convergence between African and European plates (Finetti and Del Ben 1986). The Central-Southern Apennines (Fig. 6) can be represented by structural domains displaced in geographic bands, NW-SE oriented and some tens of kilometres wide (from E to W):

1 Apulian foreland, consisting of a 6–8 km thick series of Meso-Cainozoic carbonates and representative of slope or shelf depositional facies (D'Argenio, Pescatore and Scandone 1973).
2 Bradano foredeep, consisting of terrigenous sequences increasing in thickness westward, and aged Plio-Pleistocene. They suture the tectonic contact between the external thrust front and the underplating Apulia Units.
3 The eastern (external) mountain belt, represented by extended outcrops of Meso-Cainozoic basinal units and terrigenous sequences of Mio-Pleistocene age.
4 The western (internal) mountain belt, represented by thick carbonate platforms (Meso-Cainozoic). They are a) tectonically underplaced to western nappes of oceanic or transitional provenance; b) overlapping the basinal units of the eastern chain sector.

From Lower Pliocene to the Lower Pleistocene, both the internal carbonate platform and the basinal units drifted eastward and overthrusted on the undeformed Apulian carbonate platform, which is the foreland area (Mostardini and Merlini 1986; Balduzzi *et al.* 1992).

Above them, tectonic nappes are present consisting of relics of older, internal basinal domains. They were deformed, prior to the Tyrrhenian opening, during the closure of the neo-Tethydean basin, caused by the Europe-Africa collision. Several strike-slip faults divide the chain into two main arcs. The northern one consists in thrust systems structured as embricated fans in piggy-back sequences.

Multiscale derivative analysis of the Southern Italy gravity field

The gravity data of the Southern Italian region (Fig. 7a) were extracted from the data set relative to the Bouguer Gravity Anomaly Map of Italy published by the CNR (Carrozzo *et al.* 1986; reduction density: 2.4 g/cm^3), with grid spacing of 1 km.

Let us apply now multiscale derivative analysis to the whole Southern Apennines area computing three different maps, each of them emphasizing the boundaries of structures at a specific scale ('large', 'intermediate' and 'short' scale maps) (Fedi *et al.* 2005). The large-scale map (Fig. 7b) was obtained by computing enhanced horizontal derivative (equations (5) and (6) starting from the potential as first term, considering derivatives up to $m = 6$ by using $c = 1.4$ (equation (7)). This map highlights regional patterns related to the main geological domains of the Southern Apennines. They are presumably related with deep sources, probably caused by changes in crustal thickness. The intermediate scale map (Fig. 7c) was obtained by computing enhanced horizontal derivative starting from the potential as first term, considering derivatives up to $m = 9$ and by using unit weights (no weighting). We observe westward short and arc-shaped trends, variously oriented, together with some linear trends, NE-SW oriented. Most trends within the chain seem related to structural elements and generally coincide with normal faults systems and major overthrust fronts. Eastward several long lineaments are evidenced, most of them NW-SE oriented. They are probably related to hidden regional tectonic contacts between the internal nappes and the buried Apulian foreland. The short scale map was computed starting from the gravity field as first term, calculating enhanced horizontal derivative up to $m = 9$ and by using unit weights (no weighting). This map (Fig. 7d) enhances the finest gravity source patterns. It can be noticed how the simple exclusion of the potential term from the summation shown in equation (6) allows one to emphasize the geological structures at the shortest scale.

Let us now compare multiscale derivative analysis maps in Fig. 7 with other boundary estimators to define the most suitable boundary estimators for this case, where the complex structural setting (typical of a complex thrust and fold belt system) exhibits geological patterns at more scales. To this end consider a northern sector in the investigated area (black square in Fig. 7), which is a rather complex geological district from a structural point of view and apply to the gravity field the operators Theta (Fig. 8d), hyperbolic tilt angle (Fig. 8e) and total horizontal derivative of the tilt angle (Fig. 8f). Such normalized derivatives give an efficient detection of the main structural trends existing in the area. Among them, hyperbolic tilt angle and Theta map seem to provide the best results clearly outlining some regional structures. The total horizontal derivative of the tilt angle map seems instead to depict smaller features presumably related to structural elements at a more local scale. However, it appears to be more sensitive to noise than the other two techniques.

The large-scale multiscale derivative analysis map (Fig. 8a) highlights only regional patterns. As an example, a broad low appears along the main axis of the Apennine belt. Their meaning is presumably related to density contrasts located at lower crustal depths and, maybe, to lateral changes in crustal thickness. In this case, these regional trends could be correlated to local variations of the Moho depth.

The intermediate scale multiscale derivative analysis map (Fig. 8b) outlines structural elements in agreement with the known geology and with the normalized derivative maps but also lineaments previously unrevealed. The most meaningful

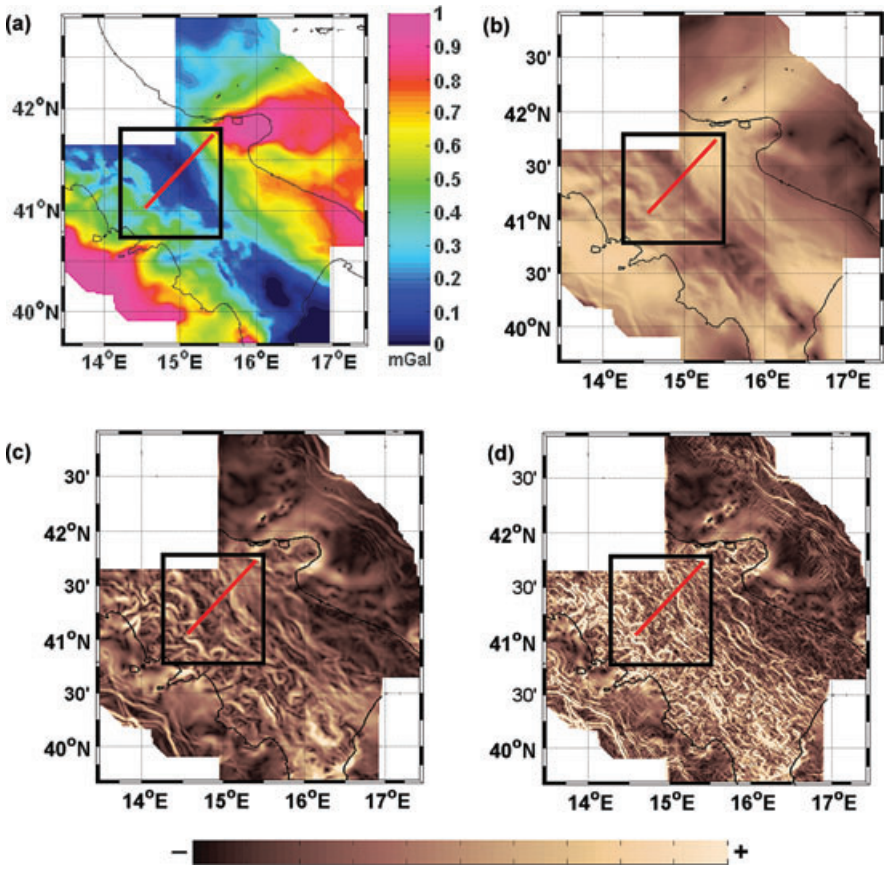

Figure 7 a) Bouguer anomaly gravity field of Southern Italy. Density for the Bouguer and terrain corrections: 2.4 g/cm^3. Normal Gravity: U.G.G.I. (1984). Reference system: IGSN71. Interpolation interval = 1 km. The black square limits the area shown in Fig. 8. The red line indicates the profile chosen to test the full multiscale approach; b) Large-scale multiscale derivative analysis map; c) intermediate scale multiscale derivative analysis map; d) short scale multiscale derivative analysis. Lineaments are defined by trends of local maxima, which are graphically determined by the colour bar shown.

lineaments bound the morpho-structural limits of the Matese massif (3; Fig. 9) and, eastward, the outcropping series of the 'Flysh Rosso', ascribed to the Lagonegro II units (4; Fig. 9). Another trend (6; Fig. 9) marks two carbonate massifs, the Camposauro (Matese-Mt.Maggiore Unit) and Mt. Taburno and Mt. Terminio (15; Fig. 9) massifs (Picentini-Taburno Unit). Westward, another trend (7; Fig. 9), marks the eastern side of Mio-Pliocenic complexes (Altavilla Unit). Finally, two trends bound the western and eastern structural limits of the carbonate series outcropping near Caserta (5; Fig. 9).

The short scale map (Fig. 8c) enhances high resolution details, mostly unrevealed by normalized derivatives. Therefore, small source boundaries are highlighted by a large number of lineaments. In the NW corner of the windowed area trends 1 and 2 (Fig. 9) appear shifted eastwards with respect to the geological limits mapped at the surface. This may indicate a structural contact running differently from that visible at the surface. A deep tectonic contact within basinal series and carbonate units (Matese Units) can be inferred. One of the largest multiscale derivative analysis lineament is an uncorrelated, long regional trend (12; Fig. 9), extending with apenninic direction from Northern Apulia to the Gulf of Taranto and precisely marking the eastern boundary of the allochtonous chain front formed since the Pliocene. Actually it is hidden by younger (Plio-Pleistocene) sediments filling the foredeep basin (Bradano Units) and outcropping from Gargano to the Taranto Gulf. Other noticeable trends (10 and 11; Fig. 9) run just west and parallel to the previous one, corresponding to buried tectonic contacts within overthrusting Irpinian and Lagonegro II Units. They reveal the existence of unit fronts during early Pliocene or Messinian. Other trends (13; Fig. 9) uncorrelated with shallow features, are oriented with the same direction within the Bradano foredeep. Near the SW corner of the windowed area a further straight E-W trend (8; Fig. 9)

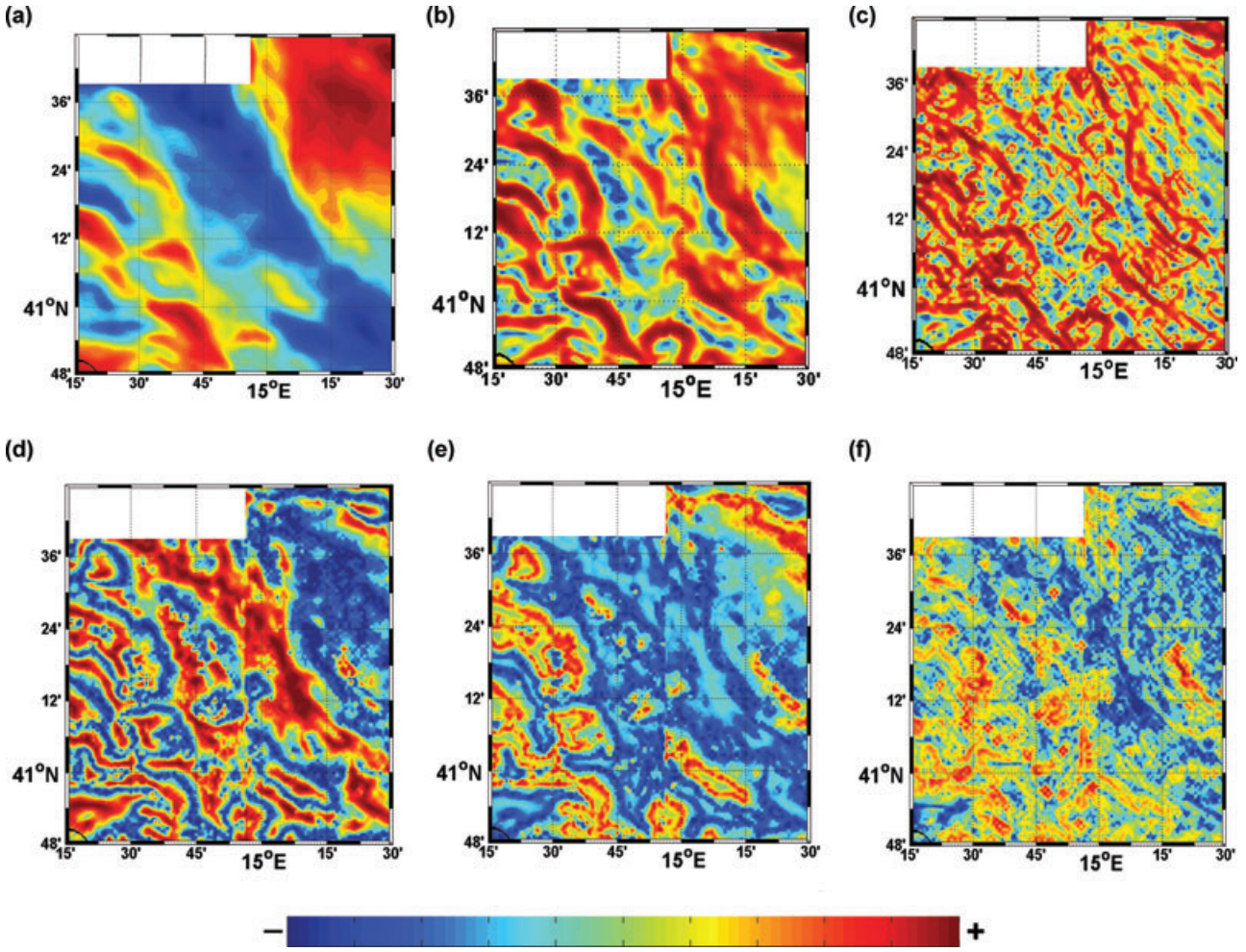

Figure 8 North-western sector of the Bouguer anomaly map of the Southern Apennine. Comparison among results provided by multiscale boundary analysis and other edge detectors based on normalized derivatives: a) large-scale multiscale derivative analysis map; b) intermediate scale multiscale derivative analysis map; c) short scale multiscale derivative analysis; d) Theta map; e) hyperbolic tilt angle map; f) total horizontal derivative tilt angle map.

runs within the Campanian plain, north of Naples. It marks a small carbonate ridge buried below the volcano-sedimentary sequences filling the Campanian plain and presumably deepening westward, beneath the volcanic cover. The multiscale derivative analysis ability to reveal fine details is shown by well-defined short scale lineaments like the trend running along the eastern side of Naples (9; Fig. 9) and coinciding with the buried morpho-structural elements of the old Sebeto valley.

Depth from extreme points application to the Southern Italy gravity field

We will therefore integrate the multiscale derivative analysis information about source boundaries with that obtained by depth from extreme points and scale function relative to the type and depth of the sources. Although the results here presented are displayed along a gravity profile crossing the main axis of the Central Apennines (red solid line, Fig. 7a), all the computations (upward continuation and vertical derivations of the field) were carried out on the whole map. The profile crosses the Apennines belt from the eastern margin of the Campanian Plain to the western margin of the Gargano Promontory. The most important units are:

a) the structural units of the Taburno-Camposauro carbonate massifs;
b) the Molise pelagic basin deposits in correspondence of the main axis of the chain;
c) the Bradano foredeep.

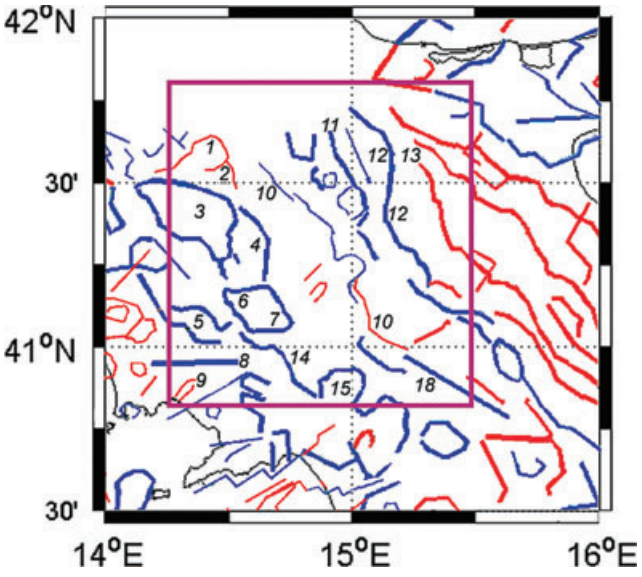

Figure 9 Major lineaments identified by enhanced horizontal derivative maxima of the intermediate scale multiscale derivative analysis of Bouguer gravity field in the studied area (black square in Fig. 7a). Blue lines: lineaments correlated with outcropping structures; red lines: uncorrelated or partially correlated lineaments. For references to the lineament numbers see the text.

The main feature of the gravity field along the profile is the long period regional negative anomaly centred on the front belt and extended along the chain axis.

As regards the large-scale, the depth from extreme points transformation was applied to the first-order derivative of the gravity field, previously upward continued to altitudes up to 20 km by means of standard techniques normally used (e.g., Baranov 1976). (Fig. 10a). The analysis of the scale function for the ridge at $x = 60$ km provided $S_2 = 1.5$ (Fig. 10b), corresponding to a source-type intermediate between a dyke-type and a cylinder-like body. The source boundaries deduced from Fig. 9(c) along the profile are reported in Fig. 10(c) and indicated with black solid lines. The depth from extreme points transformation (equation (11) was performed using the scale exponent $\alpha_2 = S_2/2 = 0.75$ and indicates a 13.2 km depth to source. From these results we can interpret the low resolution field with a large, low density body located beneath the Apennines chain at intermediate crustal depths, confirming the hypothesis of a deep crustal origin of the main negative anomaly along the belt. From a geological point of view, these features could be compatible with the hypothesis of a deep, regional folded crustal nappe (syncline) due to large-scale compressional tectonics. Its central axis could be represented by the lower terms of the carbonate series of Mesozoic age, less dense than the underlying crystalline-metamorphic basement. An alternative model (thick-skinned Tectonics), interprets this source body as a margin of the Inner Apulian carbonate platform (less dense) involved in the thrust-belt together with its crystalline-metamorphic basement (denser) (Mazzoli *et al.* 2000; Menardi Noguera and Rea 2000). This model is also compatible with our estimated structural index.

Simple tests demonstrated that bodies dipping with steep angles correspond to depth from extreme points transformed gravity fields shaped like in Fig. 10(d). Therefore, the steep westward slope of the regional source in Fig. 10(d) is consistent with the eastward direction of tectonic transport of the Apennine thrust belt at crustal scale. Note however that interference due to regional effects can also affect the shape of the depth from extreme points anomaly.

The mere qualitative analysis of the gravity field (Fig. 7a) does not reveal relevant features with local significance, even considering the limitations imposed by the 1 km sampling step. Nevertheless, the profile location through the orogenic belt should imply a much higher complexity from a structural and geological point of view. A quite complex gravity pattern should therefore be expected at a local scale, by analysing the enhanced horizontal derivative short scale map (Fig. 9c). We may see several highs corresponding to the trends of maxima intersected by our profile. Along its western end, three significant enhanced horizontal derivative highs bound two outcropping carbonate massifs, geologically ascribed to the Matese-Mt.Maggiore and Picentini-Taburno structural units ($x = 10$ km; $x = 20$ km). Moving eastward along the profile, some trends ($x = 46$, 55, 66 km) with Apenninic direction are visible. They correspond to overthrusts, along which the internal and external Irpinian Units and the Lagonegro II Unit ('Flysh Rosso') are in tectonic contact. These linear trends could probably also indicate older, buried surfaces revealing the existence of unit fronts generated during the early Pliocene or Messinian. The profile crosses a remarkable enhanced horizontal derivative trend elongated from Abruzzo to the Gulf of Taranto marking the hidden eastern boundary of the allochtonous chain front. This was formed since the Pliocene and buried beneath younger sedimentary sequences (Middle Pliocene to the Lower Pleistocene) ascribed to the foredeep basins (Bradano Units). Northward, a linear trend could be related to the presence of an inner margin of the Apulia-Gargano Platform buried by the Bradano Units.

In such case of high-resolution analysis we considered the fifth-order vertical derivative of the gravity field upward continued to altitudes up to 12 km (Fig. 11a). As previously pointed out (see also Fig. 1) such a high-order vertical derivative can be efficiently combined with upward continuation,

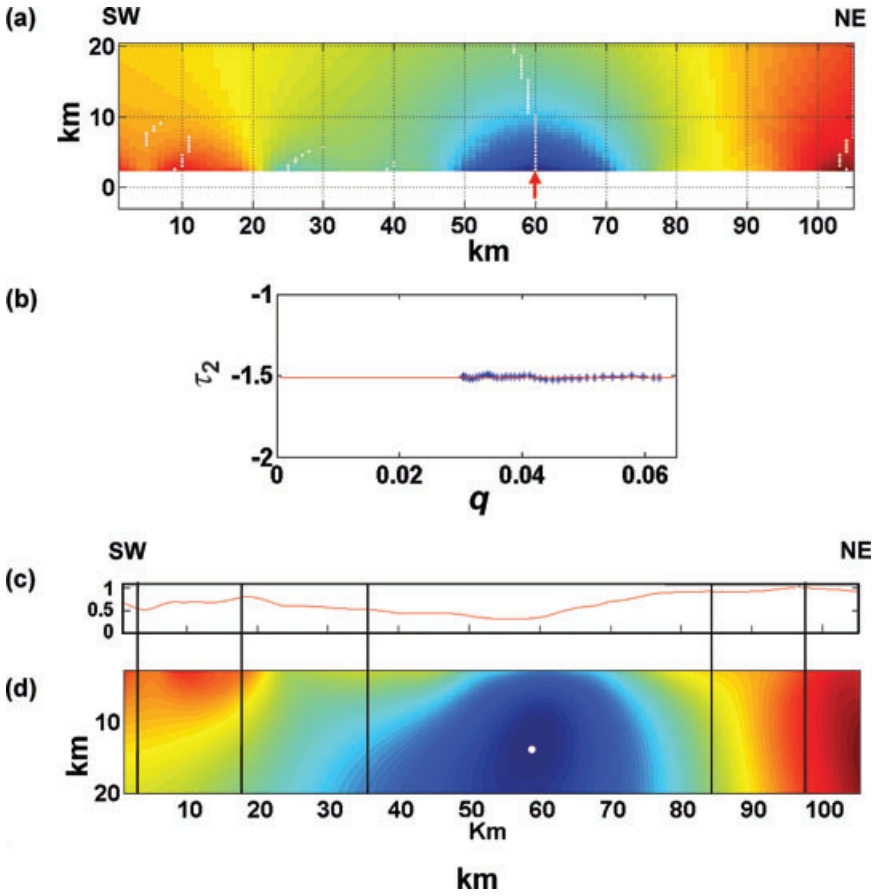

Figure 10 Integrated multiscale analysis of the gravity field along the profile shown in Figs 7 and 9(a) (regional scale): a) vertical section of the first vertical derivative of the gravity field data upward continued from 0–20 km. Ridges are also shown (white dots); b) scale function for the $x = 60$ km ridge; c) large-scale enhanced horizontal derivative signal (red line), as extracted along the section in Fig. 9(a). Enhanced horizontal derivative maxima (marked by black solid lines) locate the lateral boundaries of the sources; d) depth from extreme points transformed gravity field (first-order). Its extreme points are indicated by white dots, corresponding to the source positions.

allowing the resulting depth from extreme points transformed signal to be characterized by an acceptable signal-to-noise ratio. Hence the combined filter allowed highlighting interesting small-scale details of the gravity signal, which should refer to sources within the shallow crust. Following the graphical procedure mentioned in Fig. 4, the location of some sources can be first of all determined by a geometric method, by joining geometrically ridges in the source region (Fig. 11a, red solid lines). The scale function analysis along these ridges (according to the technique illustrated in Fig. 5) confirmed independently the depth results obtained by the geometrical method and yields about $S_6 = 6.3$ (Fig. 11b), which brings to the depth from extreme points transformation shown in Fig. 11(d), obtained by using in equation (11) the scale exponent $\alpha_6 = S_6/2$. Note the coherence between the geometrically estimated depths (whenever clear ridges may be individuated) and the depths deduced by the depth from extreme points transformation (black circles). In addition, note also the good correspondence between the position of each source identified by depth from extreme points and the boundaries deduced by the short scale multiscale derivative analysis along the profile, indicated in Fig. 11(c) by solid black lines in correspondence of the enhanced horizontal derivative maxima: the regular occurrence of the depth from extreme points between two consequent enhanced horizontal derivative highs proves the optimal integration between the two kinds of analysis. Finally, concerning the estimated type of structural index (Fig. 11b), note that it corresponds to cylinder-like sources. This should be compatible with the general morphological features of the main structures within the chain. In fact, most of them are presumably represented by thrust/fold systems variously elongated with north-eastward vergence, parallel to the belt.

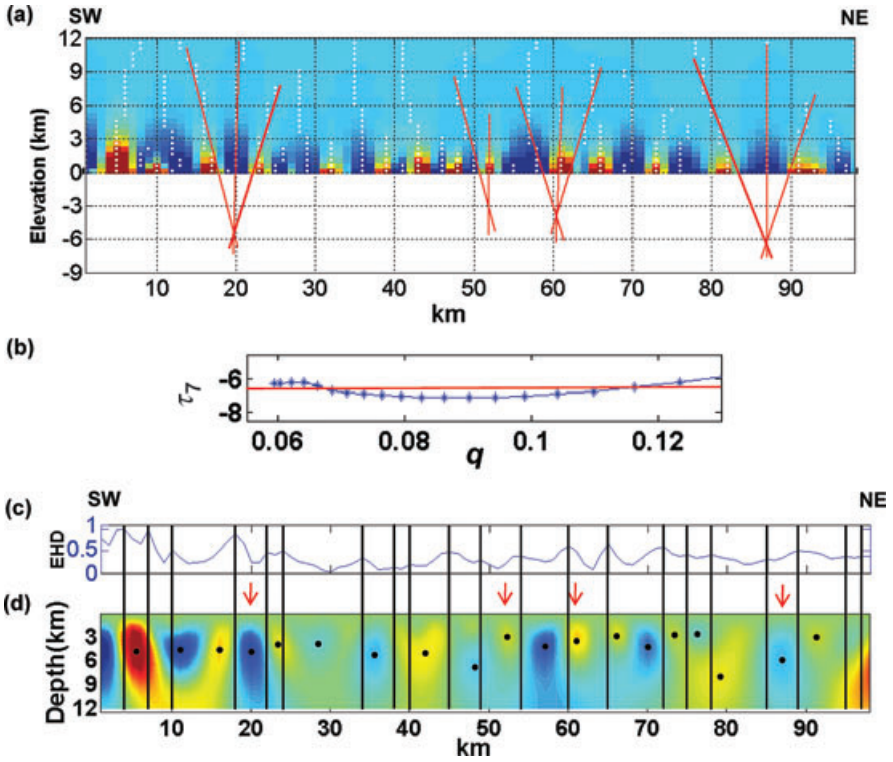

Figure 11 Integrated multiscale analysis of the gravity field along the profile shown in Figs 7 and 9(c) (local scale): a) vertical section of the fifth vertical derivative of the gravity field data upward continued from 0–12 km. Also shown ridges (white dots) and geometrical method application (red lines); b) scale function; c) small-scale enhanced horizontal derivative signal (blue line), as extracted along the section in Fig. 9(c). Enhanced horizontal derivative maxima (marked by black solid lines) locate the lateral boundaries of the sources; d) depth from extreme points transformed gravity field (fifth-order). Its extreme points are indicated by black dots, corresponding to the source positions. Red arrows indicate the analysed sources.

Therefore, they could be explained in terms of somewhat long and narrow ('cylindrical') structures. This interpretation appears more uncertain toward the ends of the profile, where different tectonic styles prevail. To the north-east (foredeep region), a thick Pliocene-Quaternary terrigenous series lay unaffected by any noticeable compressive tectonics. Along the south-western end, the profile crosses the inner side of the chain where Apennine carbonate platforms (and related foredeep deposits) outcrop with a tectonic style marked by prevailing normal fault systems. In both cases, the presence of elongated and 'cylinder-shaped' sources, causative of gravity highs and lows at depths of 3–6 km, needs alternative interpretations indicating a structural setting more complex than it was believed until now.

CONCLUSIONS

We have described a method providing a multiscale characterization of potential field sources. It is a two-step integrated application of multiscale methods, whose final result is a rather complete characterization of the sources in terms of lateral extent, depth and source-type.

The first step of our integrated method is accomplished by multiscale derivative analysis, using a boundary detection strategy that characterizes separately the anomaly sources, emphasizing their meaningful details at different scales. As the second step, the depth and the shape of these sources are estimated by means of depth from extreme points, a stable multiscale interpretation method.

We have applied this integrated approach to the gravity field of the Southern Apennines (Italy). The results achieved by multiscale derivative analysis were summarized in different maps, each of them showing the edges of anomaly sources at a different scale. As shown with synthetic examples, multiscale derivative analysis is particularly useful when the sources of the investigated area are at different scales, revealing more advantageous than other boundary analysis techniques. This is the case of the thrust and fold belt systems (e.g., the

Apennines) having a very complex structural setting and geological patterns at all scales. The better performance of multiscale derivative analysis versus normalized derivative methods (Theta, hyperbolic tilt angle and total horizontal derivative of the tilt angle) is in fact confirmed also with this set of experimental data.

Most of the geological patterns outcropping along the Apennine chain are clearly evidenced by the method. But a significant result is that several lineaments well evidenced by multiscale derivative analysis, are poorly correlated or completely uncorrelated to outcropping features. Therefore they need some interpretation because referring to geological elements hidden by shallow structures and, therefore, still unmapped.

The depth from extreme points multiscale transformation was carried out along a meaningful transect across the Central Apennines. Depth from extreme points was computed for two different scales: the first was set to reveal regional structures, the second to recognize local sources.

The analysis of the regional negative anomaly just along the Apennine axis identified a deep (13 km), low density source with structural index = 0.5, corresponding to a source-type intermediate between dyke-type and cylinder-like body. Such a body at intermediate crustal depths could be compatible with large-scale compressional tectonics causing the presence of a deep, folded crustal nappe (syncline). Its central axis could be represented by the lower terms of the carbonate series of Mesozoic age, less dense than the underlying crystalline-metamorphic basement. Nevertheless, in the frame of an alternative model (thick-skinned tectonics), this source could be interpreted as a margin of the Inner Apulian carbonate platform (less dense) involved in the thrust-belt together with the underlying crystalline-metamorphic basement (denser).

The analysis at local scale revealed the presence of somewhat long and narrow ('cylindrical') structures at a depth of 3–6 km. They seem compatible with the morphological features typical of thrust/fold systems variously elongated with north-eastward vergence and parallel to the belt. Such a model could be realistic for sources near the central axis of the Apennine chain but appears more uncertain toward the ends of the profile, where different tectonic styles prevail.

In conclusion, our integrated approach points out that a multiscale analysis is a valid tool to characterize sources of different depths and size, whose relative effects become dominant at different scales. Real sources involve obviously much more complicated distributions of density or magnetization, which may be studied with more detail when further information is available, such as other geophysical data or well-logs. Nevertheless, we have shown that the integration of methods based on very simple assumptions, e.g., idealized simple sources such as spheres, cylinders and dykes for depth from extreme points and steep sources for multiscale derivative analysis, can provide independent and valuable information about the unknown source distribution.

REFERENCES

Balduzzi A., Casnedi R., Crescenti U., Mostardini F. and Tonna M. 1982. Il Plio-Pleistocene del sottosuolo del Bacino Lucano (avanfossa appenninica). *Geologica Romana* **21**, 89–111.

Baranov W. 1976. *Potential Fields and Their Transformations in Applied Geophysics*. Gebrüder-Borntraeger.

Blakely R.J. and Simpson R.W. 1986. Approximating edges of source bodies from magnetic or gravity anomalies. *Geophysics* **51**, 1494–1498.

Carrozzo M.T., Luzio D., Margiotta C. and Quarta T. 1986. *Gravity Anomaly Map of Italy*. CNR: 'Progetto Finalizzato Geodinamica' – Sub-project: 'Modello Strutturale Tridimensionale'.

Cooper G.R.J. and Cowan D.R. 2006. Enhancing potential field data using filters based on the local phase. *Computers & Geosciences* **32**, 1585–1591.

D'Argenio B., Pescatore T. and Scandone P. 1973. Schema geologico dell'Appennino Meridionale Campania e Lucania). In: *Moderne vedute sulla geologia dell' Appennino. Problemi attuali di Scienza e di cultura, Quaderno 183*, pp. 49–72. Accademia Nazionale dei Lincei, Rome.

Fedi 2002. Multiscale derivative analysis: A new tool to enhance gravity source boundaries at various scales. *Geophysical Research Letters* **29**, 16–1–16–4.

Fedi M. 2007. DEXP: A fast method to determine the depth and the structural index of potential fields sources. *Geophysics* **72**, 1–11.

Fedi M., Cella F., Florio G. and Rapolla A. 2005. Multiscale derivative analysis of the gravity and magnetic fields of Southern Apennines (Italy). In: *CROP Deep Seismic Exploration of the Mediterranean Region* (ed. I.R. Finetti), pp. 281–318. Elsevier.

Fedi M. and Florio G. 2001. Detection of potential fields source boundaries by enhanced horizontal derivative method. *Geophysical Prospecting* **49**, 40–58.

Fedi M. and Florio G. 2002. A stable downward continuation by using the ISVD method. *Geophysical Journal International* **151**, 146–156.

Fedi M. and Florio G. 2006. SCALFUN: 3D analysis of potential field scale function to determine independently or simultaneously structural index and depth to source. 76th SEG meeting, New Orleans, Louisiana, USA, Expanded Abstracts, 963–967.

Finetti I. and Del Ben A. 1986. Geophysical study of the Tyrrhenian opening. *Bollettino di Geofisica, Teorica e Applicata* **28**, 75–156.

Florio G. and Fedi M. 2006. Euler deconvolution of vertical profiles of potential field data. 76th SEG meeting, New Orleans, Louisiana, USA, Expanded Abstracts, 958–962.

Mazzoli S., Corrado S., De Donatis M., Scrocca D., Butler R.W.H., Di Bucci D., Naso G., Nicolai C. and Zucconi V. 2000. Time and space variability of 'thin-skinned' and 'thick-skinned' thrust tectonics in the Apennines (Italy). *Rendiconti Lincei Scienze Fisische e Naturali* **11**, 5–39.

Menardi Noguera A. and Rea G. 2000. Deep structure of the Campanian–Lucanian Arc (Southern Apennine, Italy). *Tectonophysics* **324**, 239–265.

Mostardini F. and Merlini S. 1986. Appennino Centro-Meridionale. Sezioni geologiche e proposta di modello strutturale. *Memorie della Societa Geologica Italiana* **35**, 177–202.

Parotto M. and Praturlon A. 2004. The Southern Apennine Arc. In: *Geology of Italy* (eds V. Crescenti, S. D'Offizi, S. Merlino and L. Sacchi), pp. 33–58. Società Geologica Italiana, Rome.

Stavrev P.Y. 1997. Euler deconvolution using differential similarity transformations of gravity and magnetic anomalies. *Geophysical Prospecting* **45**, 207–246.

Verduzco B., Fairhead J. D., Green C.M. and Mackenzie C. 2004. New insights into magnetic derivatives. *The Leading Edge* **22**, 116–119.

Wijns C., Perez C. and Kowalczyk P. 2005. Theta map: Edge detection in magnetic data. *Geophysics* **70**, 39–43.